Available online at www.sciencedirect.com
SCIENCE DIRECT®
Chemical Physics Letters 417 (2006) 48–52
CHEMICAL PHYSICS LETTERS
www.elsevier.com/locate/cplett

# Suppression of undesired peaks due to residual intermolecular dipolar interactions in liquid NMR

Zhong Chen [a,b,*], Xiaoqin Zhu [a], Shuhui Cai [a], Jianhui Zhong [b,*]

[a] Department of Physics, State Key Laboratory of Physical Chemistry of Solid Surface, Xiamen University, Xiamen, Fujian 361005, PR China
[b] Department of Radiology, University of Rochester, Rochester, NY 14642, USA

Received 20 August 2005; in final form 18 September 2005
Available online 24 October 2005

**Abstract**

Residual intermolecular dipolar interactions may result in undesired spectral features on highly concentrated samples in liquid NMR. Although homonuclear decoupling can be employed to suppress the interactions, it may cause a strong irradiation peak, which obscures the nearby peaks. In order to overcome this shortcoming, a modified CRAZED sequence with three radio-frequency pulses was proposed. The analytical expression derived from the dipolar field treatment was employed to select proper flip angles and phase cycling. Theoretical predictions, experimental observations, and computer simulations demonstrated that the new method effectively suppresses the undesired peaks due to residual dipolar effects.


## 1. Introduction

In liquid nuclear magnetic resonance (NMR), residual intermolecular dipolar interactions in highly polarized solution originate from the dipolar couplings between distant spins. Therefore, the interactions are also referred to as distant dipolar field (DDF) effects [1–3]. The strength of DDF effects depends on several factors, including relative locations of spins, overall spatial distribution of spin magnetization, and sample shapes. In isotropic liquids, intermolecular dipolar interactions are usually averaged to zero by the fast Brownian motion [4]. However, they are retained by the spatial modulation of the magnetization in the presence of gradient field or field inhomogeneity [5,6]. Although these interactions are in general very small, they form the basis for the recently developed intermolecular multiple-quantum coherence (iMQC) technique [4,7]. Warren and co-workers [8] established the theoretical foundation for the phenomena of iMQCs. Jeener [9] established the connection between the DDFs and iMQCs. Recently, the iMQC technique has attracted growing interest in magnetic resonance imaging (MRI) [10–13] and high-resolution NMR [14–16].

On the other hand, the residual DDFs may result in undesired spurious spectral features in liquid NMR. Various techniques have been proposed to suppress these effects. Utilization of coherence-selection gradients (CSGs) along the magic-angle direction is a common technique for elimination of DDF peaks [17]. An alternative technique based on the DANTE method was also proposed [18]. The weak selective irradiation using the DANTE method may cause interferences with other pulses. Moreover, their efficiency depends on sample shape, degree of field inhomogeneity, and variation of susceptibility at the sample surface. Recently, Jeener and co-workers [19] suggested to use magic-angle spinning (MAS) scheme for the complete elimination of all DDF effects in high-resolution liquid NMR. However, the method is limited in its utility due to the lack of MAS unit in most conventional liquid spectrometers. Therefore, better dipolar decoupling schemes are highly desirable.

Invoking the idea from the method reported in [18], we achieved suppression of the DDF effects using a technique

* Corresponding authors. Fax: +86 592 2189426 (Z. Chen).
*E-mail addresses:* chenz@jingxian.xmu.edu.cn (Z. Chen), jianhui.zhong@rochester.edu (J. Zhong).

0009-2614/$ - see front matter © 2005 Elsevier B.V. All rights reserved.
doi:10.1016/j.cplett.2005.09.110

based on homonuclear decoupling during the acquisition period that was commonly used for homonuclear scalar decoupling. If $I$ spins in a two-spin system are scalarly coupled to $S$ spins, the spin–spin splitting of the $S$ signal due to $I$ spins would disappear when the Rabi frequency of homonuclear decoupling is much larger than the coupling constant $|J_{IS}|$ [20]. Since the residual intermolecular dipolar coupling is generally very small, typically about 1 Hz, it is possible to decouple the dipolar coupling using the homonuclear decoupling technique. The main problem of the technique is that a strong irradiation peak might obscure the nearby peaks. To overcome this shortcoming, we also propose a modified CRAZED sequence [4] with three radio-frequency (RF) pulses. Both experimental observations and computer simulations showed that the three-pulse sequence with proper phase cycling scheme can suppress efficiently the undesired peaks due to residual DDF effects. This method can be used to effectively suppress various iMQC signals such as the undesired intermolecular cross-peaks in 2D NMR spectra.

## 2. Theory and method

Although iMQC effects originating from higher-spin terms are readily observable at high fields, most of the iMQC applications adopt intermolecular zero-quantum or double-quantum coherences (iZQCs or iDQCs) that originate from the two-spin terms in equilibrium density matrix and generate the strongest signals in most common cases. Therefore, we pay our attention to the iZQCs and iDQCs in a two-component sample with solvent and solute denoted by $I$ and $S$, respectively. In modified CRAZED sequences shown in Fig. 1, a pair of linear gradient pulses with an area ratio of 1:−2 are applied to select iDQCs, or iMQCs of coherence order −2. The first RF pulse is non-selective. When the second RF pulse is selective for $I$ spins (or a specific peak of $S$ component), the DDFs only originate from solvent (or corresponding spins of solute).

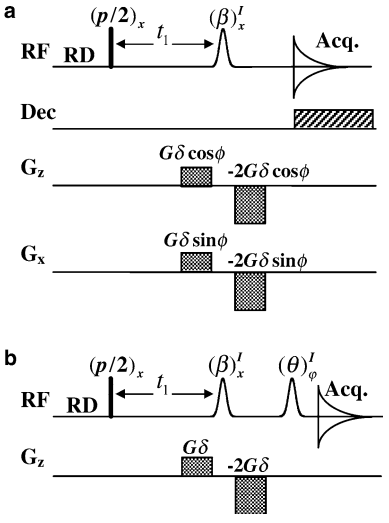


Fig. 1. Pulse sequences for suppressing the dipolar interactions by (a) homonuclear dipolar decoupling and (b) three pulses with proper phase cycling and flip angles.

The DDFs originating from solvent are taken as an example to demonstrate the theoretical description with the dipolar field treatment [8,21]. For simplicity, effects of radiation damping, relaxation, diffusion, and scalar coupling are neglected. The magnetization density at position $\mathbf{r}$ and time $t$ is represented by $\mathbf{M}(\mathbf{r}, t)$ [22]. Before the first pulse, the magnetization densities of the $I$ and $S$ spins can be written as

$$\begin{aligned}\mathbf{M}^I(\mathbf{r},0) &= M_0^I\hat{\mathbf{z}},\\ \mathbf{M}^S(\mathbf{r},0) &= M_0^S\hat{\mathbf{z}},\end{aligned} \tag{1}$$

where $M_0^I$ and $M_0^S$ represent the equilibrium magnetizations of spins $I$ and $S$ per unit volume, respectively. The unit vector $\hat{\mathbf{z}}$ is along the direction of the large external magnetic field. For the sequence shown in Fig. 1a, the magnetization densities after the second gradient pulse become [21]

$$\begin{aligned}\mathbf{M}^I(\mathbf{r},t_1+\delta^-) &= M_0^I\{-[\hat{\mathrm{y}}\cos(\Delta\omega_I\delta-2\varphi_\mathrm{g})-\hat{\mathrm{x}}\sin(\Delta\omega_I\delta-2\varphi_\mathrm{g})]\\ &\quad\times\cos\beta\cos(\Delta\omega_I t_1+\varphi_\mathrm{g})-\hat{\mathrm{z}}\sin\beta\cos(\Delta\omega_I t_1+\varphi_\mathrm{g})\\ &\quad+[\hat{\mathrm{x}}\cos(\Delta\omega_I\delta-2\varphi_\mathrm{g})+\hat{\mathrm{y}}\sin(\Delta\omega_I\delta-2\varphi_\mathrm{g})]\\ &\quad\times\sin(\Delta\omega_I t_1+\varphi_\mathrm{g})\},\\ \mathbf{M}^S(\mathbf{r},t_1+\delta^-) &= -M_0^S\{[\hat{\mathrm{y}}\cos(\Delta\omega_S t_1+\Delta\omega_S\delta+\varphi_\mathrm{g})\\ &\quad-\hat{\mathrm{x}}\sin(\Delta\omega_S t_1+\Delta\omega_S\delta+\varphi_\mathrm{g})]\exp(\mathrm{i}\Delta\omega_S\delta-\mathrm{i}2\varphi_\mathrm{g})\},\end{aligned} \tag{2}$$

where $\Delta\omega_I$ and $\Delta\omega_S$ represent the resonance offsets of $I$ and $S$ spins in the rotating frame, respectively; $\varphi_\mathrm{g}=\gamma G\delta z$ is the dephasing angle at position $z$ due to the gradient, in which $\gamma$ is the gyromagnetic ratio, and $G$ and $\delta$ are amplitude and duration of the first iMQC-selection gradient, respectively; $\beta$ is the flip angle of the second RF pulse. Considering the spatially modulated longitudinal component in Eq. (2), the effective DDF seen by $S$ spins is given by [21]

$$B_{\mathrm{d1}}^S=-\frac{2}{3}\mu_0\Delta_s M_0^I\sin\beta\cos(\Delta\omega_I t_1+\varphi_\mathrm{g}), \tag{3}$$

where $\mu_0$ is the magnetic vacuum permeability; $\Delta_s=[3(\hat{\mathrm{s}}\cdot\hat{\mathrm{z}})^2-1]/2$, in which the unit vector $\hat{\mathrm{s}}$ is along the direction of CSGs. Since the angle between the gradient field and $z$ direction is $\phi$, $\Delta_s=(3\cos^2\phi-1)/2$. When the gradient field is oriented along the $z$ direction, i.e. $\phi=0°$, we have $\Delta_s=1$. The magic-angle condition for the CSGs is determined by $3\cos^2\phi-1=0$, or $\phi=54.7°$. Since the DDFs originate from $I$ spins only, the dipolar decoupling will be realized when $I$ spins are selectively irradiated during the detection period (Fig. 1a). However, the irradiation resonance becomes very strong and the peaks close to it may be distorted. To avoid these nuisances, another RF pulse with flip angle $\theta$ is adopted immediately after the second CSG, as shown in Fig. 1b. With assumption $\beta=\pi/2$ for simplicity, after the $\theta$ pulse applied along the $x$ direction, Eq. (2) becomes

$$\begin{aligned}\mathbf{M}^I(\mathbf{r}, t_1+\delta^+) &= M_0^I\{-(\hat{\mathrm{z}}\cos\theta-\hat{\mathrm{y}}\sin\theta)\cos(\Delta\omega_I t_1+\varphi_\mathrm{g})\\ &+\hat{\mathrm{x}}\sin(\Delta\omega_I t_1+\varphi_\mathrm{g})\cos(\Delta\omega_I\delta-\mathrm{i}2\varphi_\mathrm{g}+\gamma B_{\mathrm{d}1}\delta)\\ &+(\hat{\mathrm{y}}\cos\theta+\hat{\mathrm{z}}\sin\theta)\sin(\Delta\omega_I t_1+\varphi_\mathrm{g})\\ &\times\sin(\Delta\omega_I\delta-i2\varphi_\mathrm{g}+\gamma B_{\mathrm{d}1}\delta)\},\\ \mathbf{M}^S(\mathbf{r}, t_1+\delta^+) &= -M_0^S\{[\hat{\mathrm{y}}\cos(\Delta\omega_S t_1+\Delta\omega_S\delta+\varphi_\mathrm{g})\\ &-\hat{\mathrm{x}}\sin(\Delta\omega_S t_1+\Delta\omega_S\delta+\varphi_\mathrm{g})]\\ &\times\exp(-\mathrm{i}2\varphi_\mathrm{g}+\frac{2}{3}\gamma B_{\mathrm{d}1}\delta)\}.\end{aligned} \tag{4}$$

In the following, we will focus on the signal from $S$ spins, since it is what is desired for observation in most solute–solvent systems. Considering the spatially modulated longitudinal component in Eq. (4), the effective DDFs seen by $S$ spins only originate from $I$ spins [21]

$$\begin{aligned}B_{\mathrm{d}2}^S &= -\frac{1}{3}\mu_0\Delta_s M_0^I[2\cos\theta\cos(\Delta\omega_I t_1+\varphi_\mathrm{g})\\ &+\sin\theta\cos(\Delta\omega_I t_1-\varphi_\mathrm{g})-\cos(\Delta\omega_I t_1+3\varphi_\mathrm{g})\\ &\times\sin\theta].\end{aligned} \tag{5}$$

The transverse magnetization related to $S$ spins evolves under the combined effects of the effective DDFs and angular frequency offset $\Delta\omega_S$ in the rotating frame [21]. It is noted that the DDF effects, $\exp(\mathrm{i}\gamma B_\mathrm{d}^S t_2)$, can be expressed by the expansion $\exp(\mathrm{i}\xi_n\cos\alpha)=\sum_{k=-\infty}^{\infty} i^k J_k(\xi_n)\mathrm{e}^{\mathrm{i}k\alpha}$ $(n=1, 2, 3)$, where $J_k(\xi_n)$ is the Bessel function of integer order $k$ and $\xi_n$ is the argument of the Bessel function. Thus, we have

$$\begin{aligned}M_+^S &= -\mathrm{i}M_0^S\exp(\mathrm{i}\Delta\omega_S t_2)\exp(\mathrm{i}\Delta\omega_S t_1+\mathrm{i}\Delta\omega_S\delta-\mathrm{i}\varphi_\mathrm{g})\\ &\times\sum_q i^q J_q(\xi_0)\exp(\mathrm{i}q\Delta\omega_I t_1+\mathrm{i}q\gamma GTz)\\ &\times\sum_k i^k J_k(\xi_1)\exp(\mathrm{i}k\Delta\omega_I t_1+\mathrm{i}k\varphi_\mathrm{g})\sum_l i^l J_l(\xi_2)\\ &\times\exp(\mathrm{i}l\Delta\omega_I t_1+\mathrm{i}l\Delta\omega_I\delta-\mathrm{i}l\varphi_\mathrm{g})\sum_r i^r J_r(\xi_3)\\ &\times\exp(-\mathrm{i}r\Delta\omega_I t_1+\mathrm{i}r\Delta\omega_I\delta-\mathrm{i}r3\varphi_\mathrm{g}),\end{aligned} \tag{6}$$

where

$$\begin{aligned}\xi_0 &= \frac{2}{3}\gamma\mu_0 M_0^I\Delta_s\delta,\\ \xi_1 &= -\frac{2}{3}\gamma\mu_0 M_0^I\Delta_s t_2\cos\theta,\\ \xi_2 &= -\frac{1}{3}\gamma\mu_0 M_0^I\Delta_s t_2\sin\theta,\\ \xi_3 &= \frac{1}{3}\gamma\mu_0 M_0^I\Delta_s t_2\sin\theta.\end{aligned} \tag{7}$$

Eq. (6) provides a general analytical expression for the NMR signals related to DDFs for two-component samples containing only $I$ and $S$ spins [21]. In order to evaluate the signal intensity of the whole sample, the average of the complex magnetization over all $z$ positions must be taken. If the size scale of a sample is much larger than the dipolar correlation distance of spatial modulation ($d=2\pi/(\gamma G\delta)$), the spatial averaging across the sample retains only terms with $q=1$, $k=l=r=0$; $k=1$, $q=l=r=0$; and $l=-1$, $q=k=r=0$, independent of the absolute position in the sample. The effects of sample shape can also be neglected [8]. Therefore, the resulting transverse magnetization is

$$\begin{aligned}M_+^S &= M_0^S(\gamma\mu_0\Delta_s M_0^I\delta/3)\exp(\mathrm{i}\Delta\omega_S t_2)\exp(\mathrm{i}\Delta\omega_I t_1\\ &+\mathrm{i}\Delta\omega_S t_1+\mathrm{i}\Delta\omega_S\delta)-M_0^S(\gamma\mu_0\Delta_s M_0^I t_2/3)\\ &\times\cos\theta\exp(\mathrm{i}\Delta\omega_S t_2)\exp(\mathrm{i}\Delta\omega_I t_1+\mathrm{i}\Delta\omega_S t_1\\ &+\mathrm{i}\Delta\omega_S\delta)-M_0^S(\gamma\mu_0\Delta_s M_0^I t_2/6)\sin\theta\exp(\mathrm{i}\Delta\omega_S t_2)\\ &\times\exp(-\mathrm{i}\Delta\omega_I t_1+\mathrm{i}\Delta\omega_S t_1-\mathrm{i}\Delta\omega_I\delta+\mathrm{i}\Delta\omega_S\delta).\end{aligned} \tag{8}$$

Since all experiments presented herein satisfy the condition of small DDFs, that is, $\xi_n \ll 1$ $(n=1, 2, 3)$, only zero- and first-order Bessel functions need to be considered. Moreover, the Bessel functions can be safely approximated to the first term of Tailor expansion $J_k(\xi)\cong(\xi/2)^k/k!$ in Eq. (8) [22]. The first and second terms of Eq. (8) correspond to the signal originating from iDQCs, while the third term corresponds to the signal originating from iZQCs. Since $\delta$ is very short, typically 1–2 ms, the first term is very small and can be ignored. Eq. (8) indicates that the iDQC and iZQC signals are highly sensitive to the flip angle of the third pulse, $\theta$. To detect the signal from a specific coherence, an efficient phase cycling scheme is required. When a two-step phase cycling of the form $(\theta_x, \theta_{-x})$ with the receiver phase $(x, -x)$ is used, denoted as cycle-I, the term proportional to $\cos\theta$ in Eq. (8) will be removed, leaving the term proportional to $\sin\theta$. It means that only iZQC term in Eq. (8) is retained when cycle-I is applied. When the pulse sequence shown in Fig. 1b is employed with cycle-I and $\theta=0$ or $\pi$, the signals originating from iZQCs and iDQCs are suppressed effectively. Similarly, when a two-step phase cycling of the form $(\theta_x, \theta_{-x})$ with the receiver phase $(x, x)$ is used, denoted as cycle-II, the term proportional to $\sin\theta$ in Eq. (8) will be removed, leaving the term proportional to $\cos\theta$ [23]. It means that only iDQC term in Eq. (8) is retained when cycle-II is applied. Moreover, if the flip angle $\theta$ is set to $\pi/2$ and cycle-II is used, the $S$ signals originating from iZQCs and iDQCs are suppressed effectively.

## 3. Experimental

Experiments with the pulse sequences shown in Fig. 1 were performed on a Varian INOVA 600 NMR spectrometer, equipped with self-shielded $x$, $y$, and $z$ gradient coils and a 5 mm HCN triple-resonance RF coil of 1.5 cm effective length. All experiments were recorded at 298 K. Two samples were used: a mixture of 40% methyl ethyl ketone ($CH_3CH_2COCH_3$) and 30% chloroform ($CHCl_3$), and a mixture of 40% $n$-propyl alcohol ($CH_3(CH_2)_2OH$) and 30% chloroform. 30% chloroform-$d_6$ ($CDCl_3$) was added for locking and shimming field as well as lowering the $Q$ factor and hence prolonging the radiation damping time.

To suppress the effects of radiation damping further, the width of $\pi/2$ hard pulse was extended from 6 to 70 μs by deliberately detuning the probe. The gradient amplitude and duration were $G \approx 0.1$ T/m and $\delta = 1.2$ ms. The acquisition time was 1.5 s. The widths of the selective $\pi/2$ Gaussian pulses were 3.5 ms. The relaxation delay (RD) of 40 s was used, to allow the spin system to return to its full equilibrium state and prevent any possibility of stimulated echoes.

### 3.1. Results and discussion

Fig. 2 shows the decoupling of the DDFs originating from solvent in the mixture of methyl ethyl ketone (solute, *S* spins) and chloroform (solvent, *I* spins), using the pulse sequence in Fig. 1a. Fig. 2a is the conventional one-dimensional (1D) spectrum, where A, B, and C peaks represent the $CH_2$ and $CH_3$ protons in the ethyl group and the $CH_3$ protons in the methyl group, respectively. The scalar coupling between the A and B protons splits the A peak to quartet and B peak to triplet (see the inserted spectra in Fig. 2a). D peak comes from the solvent protons. When the pulse sequence shown in Fig. 1a was applied and the second pulse was selective for the solvent (D), the 1D iDQC spectrum with the CSGs along *z* direction is given in Fig. 2b. The DDFs are caused by the D spins, which are responsible for the iDQC signals. When the *z*-direction CSGs were switched to the magic-angle direction, the peaks located at A, B, C, and D positions almost disappeared completely (see Fig. 2c), revealing that the four peaks in Fig. 2b were resulted from DDFs. The residual weak peak at the D position was possibly due to the residual conventional single-quantum signals and deviation of the CSGs from the magic-angle direction. When the experimental conditions were the same as Fig. 2b except that the D peak was selectively irradiated during the acquisition period, i.e. homonuclear decoupling, the A, B, and C peaks disappeared (see Fig. 2d). When the experimental conditions were same as Fig. 2d except that the A peak instead was selectively irradiated during the acquisition period, the four peaks originating from iDQCs still existed but the splitting between the A and B scalar coupling disappeared (see the inset in Fig. 2e). This is because that the selective irradiation was applied at the A peak while the iDQC signals are originating from the DDFs of D spins. Fig. 2d,e demonstrates that the homonuclear decoupling is effective only when the irradiation is applied selectively on the specific spins which produce the DDFs. The main shortcoming of the technique is that the strong irradiation peak might obscure the peaks nearby. Fig. 3 displays the results using the pulse sequence shown in Fig. 1b. Fig. 3a

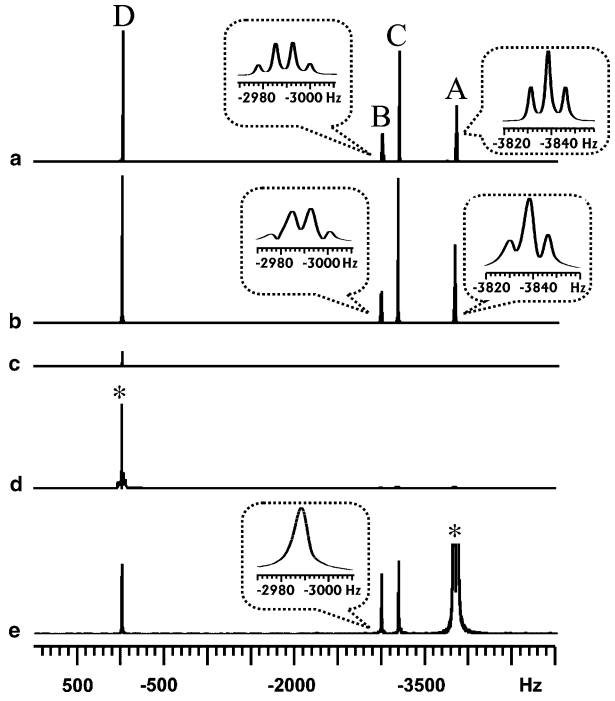


Fig. 2. Results using pulse sequence in Fig. 1a. (a) 1D conventional SQC spectrum of a mixture of methyl ethyl ketone and chloroform. (b)–(e): 1D iDQC spectra when the second RF pulse in Fig. 1a is selective for the D peaks. (b) Without homonuclear decoupling irradiation and with CSGs along the *z* direction; (c) without homonuclear decoupling irradiation and with CSGs along the magic-angle direction; (d) with homonuclear decoupling irradiation at the D peak and with CSGs along the *z* direction; (e) with homonuclear decoupling irradiation at the A peak and with CSGs along the *z* direction. The peaks marked by * are truncated due to their strong intensities. All the spectra are in the same intensity scales except for the inserted magnified spectra.

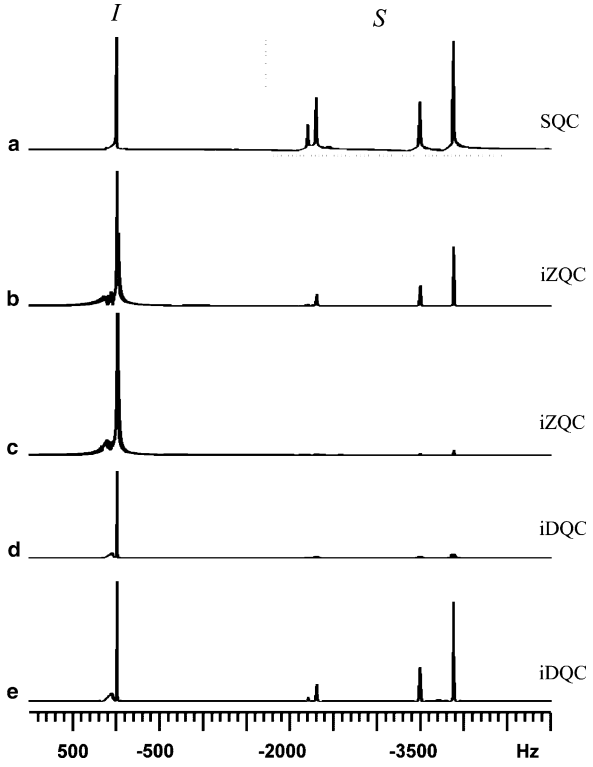


Fig. 3. Results using pulse sequence in Fig. 1b. (a) 1D conventional SQC spectrum of a mixture of *n*-propyl alcohol (*S* spins) and chloroform (*I* spins). (b)–(e): The iMQC signals of the *S* spins acquired using the pulse sequence shown in Fig. 1b with $\theta = \pi/2$ (b, iZQC), $\theta = \pi$ (c, iZQC), $\theta = \pi/2$ (d, iDQC), and $\theta = \pi$ (e, iDQC).

is the conventional 1D spectrum of the mixture of *n*-propyl alcohol (solute, *S* spins) and chloroform (solvent, *I* spins). When the phase cycle-I is applied, Eq. (8) predicts that only iZQC signals of the *S* spins, which are proportional to sin $\theta$, will be observed. The iZQC signals reach maximum at $\theta = \pi/2$ and null at $\theta = \pi$. The corresponding experiments are shown in Fig. 3b,c. When the phase cycle-II is applied, Eq. (8) predicts that only iDQC signals of the *S* spins will be observed, which is proportional to cos$\theta$ when the first term in Eq. (8) is ignored. The iDQC signals reach null at $\theta = \pi/2$ and maximum at $\theta = \pi$. The corresponding experiments are shown in Fig. 3d,e. The residual solute signals in Fig. 3c,d may be due to the imperfect flip angle $\theta$.

To quantify theoretical predictions and experimental observations, computer simulations based on the Bloch equations with an additional nonlinear term describing the DDFs [24] were performed. The parameter sets were chosen to be as close to the actual experiments as possible. Fig. 4 demonstrates the variation of the $^1$H signal amplitudes of *S* spins (the $CH_3$ protons in *n*-propyl alcohol) with the flip angle $\theta$ from 0 to $2\pi$ in an increment of $\pi/20$. The symbols '○' indicate the experimental observation of iZQC signals, '▲' indicate the simulated data of iZQC signals. '▽' indicate the experimental observation of iDQC signals, and '☆' indicate the simulated data of the iDQC signals. The solid line is based on the theoretical expression, sin$\theta$, for iZQCs, and the dot line is based on the theoretical expression, cos$\theta$, for iDQCs, respectively. When the cycle-I scheme was used and $\theta = k\pi$ ($k = 0, 1, 2, \ldots$), the iZQC signals were effectively suppressed. When the cycle-II scheme was used and $\theta = (2k+1)\pi/2$ ($k = 0, 1, 2, \ldots$), the iDQC signals were effectively suppressed. The small residual signal at $\theta = \pi/2$ may be corresponding to the first term of Eq. (8).

The method proposed herein can effectively suppress the iDQCs and iZQCs of *S* spins originating from DDF effects caused by solvent. It is helpful for a better understanding of the residual dipolar coupling. Based on the method, new pulse sequences may be designed to effectively suppress the various iMQC signals such as the undesired intermolecular cross-peaks in 2D NMR spectra [22].

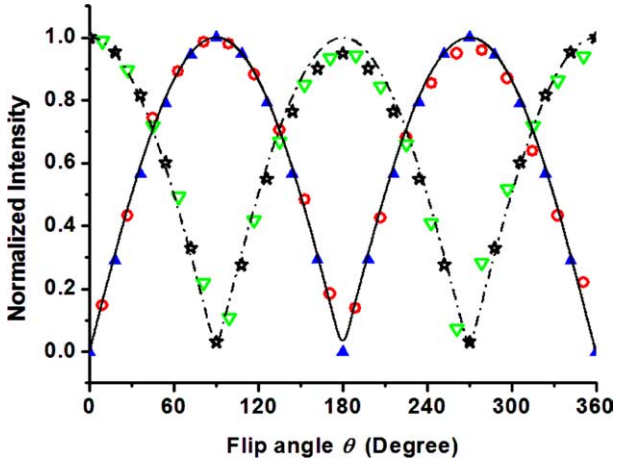


Fig. 4. Variation of $^1$H signal amplitudes of *S* spins (the $CH_3$ protons in *n*-propyl alcohol) with the flip angle $\theta$ using pulse sequence in Fig. 1b.

## 4. Conclusion

The homonuclear decoupling technique can be used to effectively suppress the residual DDFs in highly polarized liquid NMR, but it may result in a strong irradiation peak with a broad baseline. A modified CRAZED sequence with three RF pulses was proposed to overcome this shortcoming. The analytical expression derived from the dipolar field treatment was used to determine proper flip angle and phase cycling. Both experimental and simulated results are in good agreement with the theoretical predictions.

## Acknowledgments

This work was supported by the NNSF of China under Grants 10234070 and 10375049, NCET and EYTP of Ministry of Education of China, and the NIH of USA under Grant NS41048.

## References

[1] S. Capuani, R.T. Branca, M. Alesiani, B. Maraviglia, Appl. Magn. Reson. 27 (2004) 321.
[2] C.A. Corum, A.F. Gmitro, J. Magn. Reson. 171 (2004) 131.
[3] M.P. Ledbetter, I.M. Savukov, M.V. Romalis, Phys. Rev. Lett. 94 (2005) 060801.
[4] W.S. Warren, W. Richter, A.H. Andreotti, B.T. Farmer II, Science 262 (1993) 2005.
[5] E. Brunner, Concepts Magn. Reson. 13 (2001) 238.
[6] C.A. Corum, A.F. Gmitro, in: Proceedings of the International Society of Magnetic Resonance in Medicine 12th Scientific Meeting, Kyoto, 2004, p. 2711.
[7] J. Jeener, in: D.M. Grant, R.K. Harris (Eds.), Encyclopedia of Nuclear Magnetic Resonance, vol. 9, Wiley, New York, 2002, p. 642.
[8] S. Lee, W. Richter, S. Vathyam, W.S. Warren, J. Chem. Phys. 105 (1996) 874.
[9] J. Jeener, J. Chem. Phys. 116 (2002) 1204.
[10] S. Capuani, R.T. Branca, A. Alesiani, B. Maraviglia, Magn. Reson. Imaging 21 (2003) 413.
[11] J. Zhong, Z. Chen, E. Kwok, Magn. Reson. Med. 43 (2000) 335.
[12] S. Capuani, F. Curzi, F.M. Alessandri, B. Maraviglia, A. Bifone, Magn. Reson. Med. 46 (2001) 683.
[13] W.S. Warren, S. Ahn, M. Mescher, M. Garwood, K. Ugurbil, W. Richter, R.R. Rizi, J. Hopkins, J.S. Leigh, Science 281 (1998) 247.
[14] Y.Y. Lin, S. Ahn, N. Murali, W. Brey, C.R. Bowers, W.S. Warren, Phys. Rev. Lett. 85 (2000) 3732.
[15] Z. Chen, Z.W. Chen, J. Zhong, J. Am. Chem. Soc. 126 (2004) 446.
[16] S. Vathyam, S. Lee, W.S. Warren, Science 272 (1996) 92.
[17] D.L. Mattiello, W.S. Warren, L. Mueller, B.T. Farmer, J. Am. Chem. Soc. 118 (1996) 3253.
[18] P. Broekaert, A. Vlassenbroek, J. Jeener, G. Lippens, J.M. Wieruszeski, J. Magn. Reson. A 120 (1996) 97.
[19] P. Broekaert, J. Jeener, G. Lippens, J.M. Wieruszeski, J. Magn. Reson. 145 (2000) 259.
[20] R. Freeman, Spin Choreograph: Basic Steps in High Resolution NMR, Oxford University Press, Oxford, New York, 1998.
[21] Z. Chen, Z.W. Chen, J. Zhong, J. Chem. Phys. 115 (2001) 10769.
[22] Z. Chen, Z.W. Chen, J. Zhong, J. Chem. Phys. 117 (2002) 8426.
[23] J.P. Marques, R. Bowtell, Magn. Reson. Med. 51 (2004) 148.
[24] C.B. Cai, Z. Chen, S.H. Cai, J. Zhong, J. Magn. Reson. 172 (2005) 242.